

Journal of Mechanics

<http://journals.cambridge.org/JOM>

Additional services for *Journal of Mechanics*:

Email alerts: [Click here](#)

Subscriptions: [Click here](#)

Commercial reprints: [Click here](#)

Terms of use : [Click here](#)



Dynamic Analysis and Preliminary Evaluation of a Spring-Loaded Upper Limb Exoskeleton for Resistance Training with Overload Prevention

T.-M. Wu and D.-Z. Chen

Journal of Mechanics / Volume 29 / Issue 01 / March 2013, pp 35 - 44

DOI: 10.1017/jmech.2012.141, Published online:

Link to this article: http://journals.cambridge.org/abstract_S1727719112001414

How to cite this article:

T.-M. Wu and D.-Z. Chen (2013). Dynamic Analysis and Preliminary Evaluation of a Spring-Loaded Upper Limb Exoskeleton for Resistance Training with Overload Prevention. Journal of Mechanics, 29, pp 35-44 doi:10.1017/jmech.2012.141

Request Permissions : [Click here](#)

DYNAMIC ANALYSIS AND PRELIMINARY EVALUATION OF A SPRING-LOADED UPPER LIMB EXOSKELETON FOR RESISTANCE TRAINING WITH OVERLOAD PREVENTION

T.-M. Wu D.-Z. Chen *

*Department of Mechanical Engineering
National Taiwan University
Taipei, Taiwan 10617, R.O.C.*

ABSTRACT

Resistance training has been shown to be effective for developing musculoskeletal strength and is recommended by many major health organizations, such as the American College of Sports Medicine and the American Heart Association. This form of training is available for most populations, including adolescents, healthy adults, the elderly, and the clinical population. Resistance training equipment design relies heavily on the analysis of human movement. Dynamic models of human movement help researchers identify key forces, movements, and movement patterns that should be measured. An at-home resistance training upper limb exoskeleton has been designed with a three-degree-of-freedom shoulder joint and a one-degree-of-freedom elbow joint to allow movement of the upper limb at single and multiple joints in different planes. The exoskeleton can continuously increase the resistance as the spring length changes to train more muscle groups and to reduce the potential risk of muscle injury to the upper limb by free weights and training equipment. The objectives of this research were to develop a dynamic model of the spring-loaded upper limb exoskeleton and to evaluate this model by adopting an appropriate motion analysis system to verify our hypotheses and to determine the optimal configuration of a spring-loaded upper limb exoskeleton for further verification studies.

Keywords: Exoskeleton, Resistance training, Upper limb, Motion analysis.

1. INTRODUCTION

Resistance training is a common activity for young adults, athletes, and body builders, who are healthy enough to improve muscular strength, size, athletic performance, and overall physical conditioning. It is also an effective method for developing musculoskeletal strength and is recommended by many major health organizations, such as the American College of Sports Medicine and the American Heart Association [1-4]. In fact, resistance exercise has grown in popularity for many groups, including adolescents, healthy adults, the elderly, and clinical populations. Incorporating individualized, progressive resistance training programs can reduce risk factors associated with cardiopulmonary, musculoskeletal, neuromuscular, and gerontology diseases. However, there are concerns about the negative effects and the safety of resistance exercise as a form of physical therapy when using resistance equipment or free weights.

Free weights (*e.g.*, barbells, dumbbells, and weighted balls) and weight machines are the most familiar forms of resistance tools for muscle training. The user's needs or patient's disability level influences the type of resistance tool chosen. Weight machines have been

considered to be safer to use and easier to manipulate, while free weights are more difficult to master and are more likely to cause injuries. New data suggest that sprains/strains account for approximately 46% of injuries, 90% of which are caused by free weights. Muscle strain typically results from overloading a passive muscle (*i.e.*, placing too much stress on the engaged muscle fibers) or dynamically overloading an active muscle, either in concentric or eccentric action; nonurgent muscular strains and ligamentous sprains account for 46% ~ 60% of all acute injuries in strength training. Repetitive overloading of tendons may lead to tendinitis, and although the mechanisms of muscle cramps are not fully understood, most cramps occur in a shortened muscle and are characterized by abnormal electrical activity [5-7]. Machines help stabilize the body, limit the movement around specific joints that are involved in synergy, and focus the activation to a specific set of prime movers. Conversely, free weights create a pattern of intra- and intermuscular coordination that mimics the movements of specific tasks [2].

This work describes an at-home spring-loaded upper limb resistance training exoskeleton design. This exoskeleton features a three-degree-of-freedom (3-DOF) shoulder joint and a one-degree-of-freedom (1-DOF)

* Corresponding author (dzchen@ntu.edu.tw)

elbow joint that are optimally arranged to mimic the natural upper limb movement of the GH joint: Horizontal flexion-extension (flx-ext), abduction-adduction (abd-add), flexion-extension, and elbow joint flexion-extension, allowing the limb to move using single and multiple joints in different planes. Instead of increasing the external weights stepwise in free-weight exercises, this device uses zero-free-length springs, *i.e.*, linear extension springs, in which the force is proportional to the length of the spring rather than to its elongation, allowing the resistance training exoskeleton to theoretically increase the resistance continuously by adjusting the spring length. Gradually changing the resistance allows for progressive training of more muscle groups and reduces the potential risk of injury to the upper limb skeletal muscle and joint caused by a large moment of inertia [8]. However, only a kinematic model and the derived design constraints have been established. When designing exercise devices or rehabilitation aids, using an analytical and dynamic model of human movement helps identify the key forces, movements, and movement patterns that should be measured. This movement model provides a foundation that can serve as the basis for an experimental approach and that can be used to evaluate the efficacy of the initial experimental data. The equations of motion not only provide a critical understanding of the forces experienced by a joint and an effective model of normal joint function and injury mechanics, but they also provide an initial, theoretical understanding of the actual biodynamic system and can help determine the important dynamic properties that should be measured experimentally [9-11]. Many methods have been used to derive the dynamic equations of motion that describe the dynamic behavior of the upper limb, such as the Lagrange-Euler method [12,13], the Newton-Euler method [14,15], the generalized D'Alembert principle [16,17], and Kane's method [18,19]. The most widely used methods for formulating the motion equations of multibody dynamic systems are based on the Lagrange-Euler and Newton-Euler methods.

Quantitative motion analyses of the upper limb have drawn significant attention in the past 20 years. This interest has been motivated by different goals. The availability and improvement in commercial human movement detection and tracking systems have enabled upper limb tracking [20-26]. Schmidt *et al.* [27] proposed a measurement procedure to obtain accurate joint rotation of the free wrist and elbow movement by tracking three non-collinear surface markers on each limb segment. Biryukova *et al.* [28] developed a method for reconstructing the kinematics of a human upper limb—consisting of the upper arm, forearm, and hand—based on the recordings of a spatial tracking system. Prokopenko *et al.* [29] further assessed the accuracy of the arm kinematics model proposed by Biryukova *et al.* for describing voluntary movement. Hingtgen *et al.* [30] suggested a 3-DOF shoulder joint and a 2-DOF elbow joint upper extremity kinematic model and demonstrated the effectiveness of the model by employing a Vicon motion analysis system [31] to quantify the differences between the affected and unaf-

ected upper extremity motion patterns in eight stroke patients. Conversely, Romilly *et al.* [32] attempted to assess the necessary user requirements and to determine the optimal configuration of a powered upper limb orthotic prior to prototype construction, whereas most previous studies paid more attention to the range of motion, joint angles, angular velocity/acceleration, error estimation, and the soft tissue artifacts. Most of the differences were compared between normal and impaired subjects. We conducted our experiments by measuring the shoulder and elbow joint torques during designated movements (free-weight exercise: Lateral raise, front raise, and elbow curl motion; upper limb exoskeleton: Shoulder abd-add, flx-ext, and elbow flx-ext) and compared them to the movements with free weights using an exoskeleton.

The objectives of this research were to develop a dynamic model to determine the required additional design constraints and the optimal configuration of a spring-loaded upper limb exoskeleton. It was hypothesized that with zero-free-length springs the spring-loaded upper limb exoskeleton was capable of reducing unfavorable lengthening of the muscles during high-intensity free-weight exercises. The motion analysis system was employed to investigate the upper limb kinematics in the given motions, which enables us to calculate kinetics and kinematics parameters during the designated movements performed with dumbbell and with upper limb exoskeleton. Additionally, we developed proper evaluation procedures to ensure continuous and effective data collection from a larger sample of the population in the ongoing verification studies.

2. METHODS OF SOLUTION

2.1 Dynamic Model of the Upper Limb

The Lagrange approach was used in this study to derive the equations of motion for the spring-loaded upper limb exoskeleton because it uses fewer parameters to describe a given system and to determine that these motions were mechanically analogous to the free-weight exercises.

Figure 1 shows the motion of an upper arm and forearm system. The upper arm segment is pictured from the GH joint S to the elbow joint E , whereas the forearm segment extends from the elbow joint E to the middle of the palm of the hand H . Several potential limitations of this study should be noted. First, the hand was assumed to be a rigid segment in the extension of the forearm, which means that wrist motion was not included in our study. The hand is usually held in a neutral position during forearm movements. Therefore, the gravitational variation due to the wrist motion is negligible, and the upper limb can be modeled as a two-link linkage. Second, this model assumes that the length of each segment remains constant, that each segment or link has a fixed mass that is concentrated at its center of mass, and that the location of each center of mass remains fixed during the movement. Third, the joints in the model are considered to be frictionless

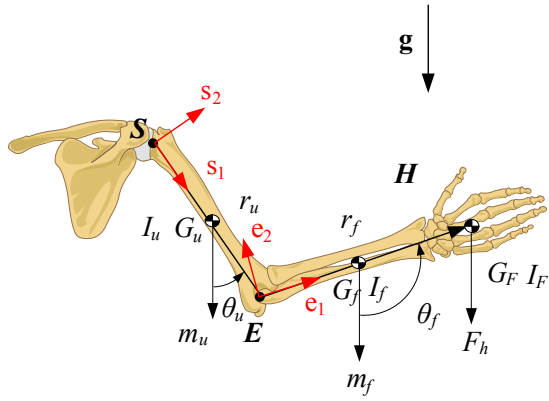


Fig. 1 The dynamic model and the coordinate system of the right upper limb

revolute joints. Fourth, the mass moment of inertia of each segment is constant during the movement. Finally, the geometries of the upper arm and the forearm were assumed to be axially symmetric. The segmental lengths of the upper arm and the forearm are denoted as r_u and r_f , respectively. The variable g denotes the gravitational force; points G_u , G_f , and G_F identify the center of gravity of the upper arm, forearm segment, and external load, respectively; and m_u , m_f , and F_h denote the mass of the upper arm, forearm segment, and external load, respectively. The mass of the human hand was ignored because it is relatively light compared to the overall mass of the upper limb. The segments were connected as a revolute joint and had three axes of rotation in the shoulder joint, including the shoulder's horizontal flx-ext, abd-add, and flx-ext, and one axis of rotation in the elbow, which provided only elbow flx-ext. An orthogonal coordinate system defined by s_1 , s_2 , and s_3 was fixed at point S and was allowed to rotate about the s_3 axis so that the unit vector s_1 always lies on segment SE . An orthogonal coordinate system defined by e_1 , e_2 , and e_3 was defined at point E and was allowed to rotate about the e_3 axis so that the unit vector e_1 always lies on segment EH . θ_u and θ_f are the angles between the segment and the vertical axis (Fig. 1).

A system with n degrees of freedom has n generalized coordinates, denoted as q_i , where i has values from 1 to n . A generalized nonconservative force corresponding to a specific generalized coordinate is represented by Q_i and the derivative of q_i with respect to time is represented as \dot{q}_i . Equation (1) shows the general form of Lagrange's equation:

$$\frac{d}{dt} \left(\frac{\partial L}{\partial \dot{q}_i} \right) - \frac{\partial L}{\partial q_i} = Q_i \quad i = 1, 2, \dots, n \quad (1)$$

The Lagrangian L is defined as the difference between the total kinetic energy T and the total potential energy V :

$$L = T - V \quad (2)$$

2.2 Dynamic Joint Torques During Free-Weight Exercise

The total kinetic energy T of the upper limb can be determined by summing the upper arm kinetic energy T_u , the forearm kinetic energy T_f , and the applied load T_F , while the total potential energy V can be determined by summing the upper arm potential energy V_u , the forearm potential energy V_f , and the applied load potential energy V_F . The equations of motion are then obtained by applying Lagrange's Eq. (1) and using the two generalized coordinates for the two-segment system, $q_1 = \theta_u$ and $q_2 = \theta_f$.

For the first generalized coordinate, $q_1 = \theta_u$, the equation of motion is determined to be

$$\begin{aligned} \tau_u = & \left[I_{u,s3} + (m_u \zeta^2 + m_f + F_h) r_u^2 \right] \ddot{\theta}_u \\ & + (m_f \xi + F_h) r_u r_f \ddot{\theta}_f \cos(\theta_f - \theta_u) \\ & - (m_f \xi + F_h) r_u r_f \dot{\theta}_f^2 \sin(\theta_f - \theta_u) \\ & + (m_u \zeta r_u + m_f r_u + F_h r_u) g \sin \theta_u \end{aligned} \quad (3)$$

For the second generalized coordinate, $q_2 = \theta_f$, the equation of motion is determined to be

$$\begin{aligned} \tau_f = & \left[I_{f,e3} + I_{F,e3} + (m_f \xi^2 + F_h) r_f^2 \right] \ddot{\theta}_f \\ & + (m_f \xi + F_h) r_u r_f \ddot{\theta}_u \cos(\theta_f - \theta_u) \\ & + (m_f \xi + F_h) r_u r_f \dot{\theta}_u^2 \sin(\theta_f - \theta_u) \\ & + (m_f \xi r_f + F_h r_f) g \sin \theta_f \end{aligned} \quad (4)$$

where τ_u is the moment at the upper arm and τ_f is the moment at the forearm. The first derivatives of θ_u and θ_f with respect to time are represented as $\dot{\theta}_u$ and $\dot{\theta}_f$. The second derivatives of θ_u and θ_f with respect to time are represented as $\ddot{\theta}_u$ and $\ddot{\theta}_f$, where $I_{u,s3}$ is the s_3 component for the mass moment of inertia about point G_u in the s_1 , s_2 , and s_3 coordinate system. $I_{f,e3}$ and $I_{F,e3}$ are the e_3 components for the mass moment of inertia about points G_f and G_F in the e_1 , e_2 , and e_3 frame of reference, respectively. The variables ζ and ξ are the ratios of the longitudinal position of the center of mass for the upper arm and the forearm segments, respectively, and they are defined as percentages of the upper arm and the forearm segments length. The ratios were 0.5772 and 0.4574 for the male subject and 0.5754 and 0.4559 for the female subject [33]. ζr_u gives the length from the mass center of the upper arm to the shoulder joint; ξr_f represents the approximate length from the mass center of the forearm to the elbow joint.

2.3 Dynamic Joint Torques with the Upper Limb Exoskeleton

Figure 2 illustrates a spring-loaded upper limb exoskeleton. The exoskeleton is assumed to be well aligned with the upper arm and has the same motion along with the upper arm.

Therefore, the angular displacement of link 3 is determined to be the same as the upper arm, that is, θ_u

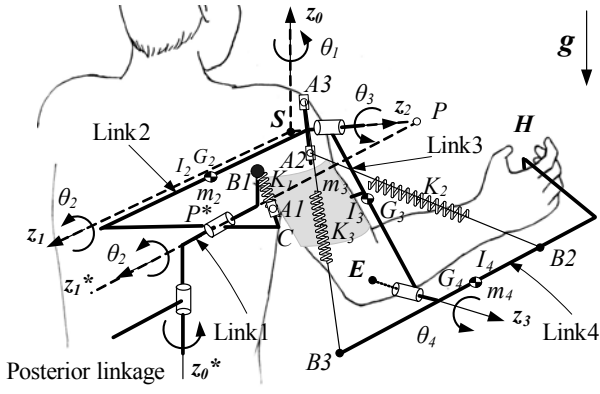


Fig. 2 A schematic diagram of the spring-loaded exoskeleton

equals θ_2 for the shoulder abd-add and θ_u equals θ_3 for the shoulder flx-ext. The angular displacement of link 4 is determined to be the same as the forearm, that is, θ_f equals θ_4 for the elbow flx-ext. Link 1 remains in its position during the exoskeleton movements.

The total kinetic energy of the upper limb exoskeleton can be determined by summing the upper arm kinetic energy T_u , the forearm kinetic energy T_f , the link 2 kinetic energy T_{L2} , the link 3 kinetic energy T_{L3} , and the link 4 kinetic energy T_{L4} . The total potential energy of the upper limb exoskeleton can be determined by summing the upper arm potential energy V_u , the forearm potential energy V_f , the link 2 potential energy V_{L2} , the link 3 potential energy V_{L3} , the link 4 potential energy V_{L4} , the K_1 spring potential energy V_{S1} , the K_2 spring potential energy V_{S2} , and the K_3 spring potential energy V_{S3} .

The equations of motion are then obtained by applying Lagrange's Eqs. (1) and (2) and by using the two generalized coordinates of the two-segment system, $q_1 = \theta_u$ and $q_2 = \theta_f$.

For the first generalized coordinate, $q_1 = \theta_u$, the equations of motion for the spring-loaded upper limb exoskeleton are determined as follows:

$$\begin{aligned}
 M_u = & \left[I_{u,s3} + I_{G2,s3} + I_{G3,s3} + (m_u \zeta^2 + m_f) r_u^2 \right. \\
 & \left. + (m_2 l_{2,G2/S}^2 + 1/4 m_3 l_3^2 + m_4 l_4^2) \right] \ddot{\theta}_u \\
 & + (m_f \xi r_u r_f + 1/2 m_4 l_3 l_4) \ddot{\theta}_f \cos(\theta_f - \theta_u) \\
 & - (m_f \xi r_u r_f + 1/2 m_4 l_3 l_4) \dot{\theta}_f^2 \sin(\theta_f - \theta_u) \\
 & + (m_u \zeta r_u + m_f r_f + m_2 l_{2,G2/S}^2 + 1/2 m_3 l_3 + m_4 l_4) g \sin \theta_u \\
 & - K_1 l_{PB1} (l_{CA1} \cos \theta_u - l_{CP} \sin \theta_u) \\
 & + (K_2 l_{SA2} - K_3 l_{SA3}) r_u \sin \theta_u \\
 & + (K_2 l_{EB2} l_{SA2} + K_3 l_{EB3} l_{SA3}) \sin(\theta_u + \theta_f)
 \end{aligned} \quad (5)$$

For the second generalized coordinate, $q_2 = \theta_f$, the equation of motion is determined as follows:

$$\begin{aligned}
 M_f = & \left[I_{f,e3} + I_{G4,e3} + m_f \xi^2 r_f^2 + 1/4 m_4 l_4^2 \right] \ddot{\theta}_f \\
 & + (m_f \xi r_u r_f + 1/2 m_4 l_3 l_4) \ddot{\theta}_u \cos(\theta_f - \theta_u) \\
 & + (m_f \xi r_u r_f + 1/2 m_4 l_3 l_4) \dot{\theta}_u^2 \sin(\theta_f - \theta_u) \\
 & + (m_f \xi r_f + 1/2 m_4 l_4) g \sin \theta_f \\
 & - (K_2 l_{EB2} - K_3 l_{EB3}) r_u \sin \theta_f \\
 & + (K_2 l_{EB2} l_{SA2} + K_3 l_{EB3} l_{SA3}) \sin(\theta_u + \theta_f)
 \end{aligned} \quad (6)$$

where M_u is the moment at the upper arm (with the exoskeleton) and M_f is the moment at the forearm (with the exoskeleton). $I_{G2,s3}$, $I_{G3,s3}$, and $I_{G4,s3}$ are the s_3 and e_3 components of the mass moment of inertia about the center of mass for link 2 (point G_2) and for link 3 (point G_3) in s_1, s_2 , and s_3 , and the center of mass for link 4 (point G_4) in the e_1, e_2 , and e_3 frame of reference. The variables m_2, m_3 , and m_4 denote the mass of link 2, link 3, and link 4, respectively, and were assumed to be fixed and located on the center lines with respect to link 2, link 3, and link 4. $l_{2,G2/S}$ is the link length between point G_2 and shoulder joint of link 2. l_3 , and l_4 represent the link lengths between two joints.

2.4 Dynamic Joint Torques During Resistance Training

2.4.1 Shoulder Abduction/Adduction

A lateral raise was used as an example of the shoulder abd-add resistance exercise used to strengthen the deltoid, latissimus dorsi, pectoralis major, supraspinatus, and trapezius muscles. In the dynamic model, the angle $\theta_f = \theta_u$. Thus, the upper arm and forearm can be considered a single link; the mass moments of inertia $I_{u,s3}$, $I_{f,e3}$, and $I_{f,s3}$ should be replaced by $I_{u/s,s3}$, $I_{f/s,s3}$, and $I_{f/s,s3}$, which are the mass moments of inertia for the upper arm, forearm, and external load with respect to the shoulder joint and are determined using the parallel axis theorem. Finally, the rotation about axis z_1^* applies to θ_2 alone, and the shoulder joint torque for θ_2 is expressed as

$$\begin{aligned}
 \tau_{2,lr} = & \left[I_{u/s,s3} + I_{f/s,s3} + I_{F/s,s3} + (m_u \zeta^2 + m_f + F_h) r_u^2 \right. \\
 & \left. + (m_f \xi^2 + F_h) r_f^2 + 2(m_f \xi + F_h) r_u r_f \right] \ddot{\theta}_u \\
 & - (m_u \zeta r_u + m_f r_u + F_h r_u + m_f \xi r_f + F_h r_f) g \sin \theta_u
 \end{aligned} \quad (7)$$

The joint torques for the shoulder using the exoskeleton are obtained by substituting the same angles for the lateral raising motion into Eqs. (5) and (6). The mass moments of inertia of links 2, 3, and 4— $I_{G2,s3}$, $I_{G3,s3}$, and $I_{G4,e3}$ —should be replaced by the mass moments of inertia with respect to the shoulder joint— $I_{G2/s,s3}$, $I_{G3/s,s3}$, and $I_{G4/s,s3}$ —using the parallel axis theorem. The potential energy of the spring depends on the movement taken because different springs are actuated depending on the movement. Only spring K_1 is actuated in the shoulder abd-add movement. The joint torque of the shoulder with the exoskeleton can be expressed as

$$\begin{aligned}
M_{2,lr} = & \left[I_{u/S,S3} + I_{f/S,S3} + I_{G2/S,S3} + I_{G3/S,S3} \right. \\
& + I_{G4/S,S3} + (m_u \zeta^2 + m_f) r_u^2 + m_f \xi^2 r_f^2 \\
& + 2m_f \xi r_u r_f + m_2 l_{2,G2/S}^2 + 1/4m_3 l_3^2 \\
& + m_4 l_3^2 + 1/4m_4 l_4^2 + m_4 l_3 l_4 \left. \right] \ddot{\theta}_u \\
& + (m_u \zeta r_u + m_f r_u + m_f \xi r_f + m_2 l_{2,G2/S}^2 \\
& + 1/2m_3 l_3 + 1/2m_4 l_4 + m_4 l_3) g \sin \theta_u \\
& - K_1 l_{PB1} (l_{CA1} \cos \theta_u - l_{CP} \sin \theta_u) \quad (8)
\end{aligned}$$

2.4.2 Shoulder Flexion/Extension

An example of the shoulder flx-ext resistance exercise is the frontal raise, which strengthens the deltoid, the pectoralis major, the latissimus dorsi, and the trapezius muscles. In the dynamic model, the angle $\theta_f = \theta_u$. The upper arm and forearm are considered to be a single rigid body rotating about the z_2 axis with an angle θ_3 . Therefore, the mass moments of inertia $I_{u,S3}$, $I_{f,e3}$, and $I_{F,e3}$ should be replaced by $I_{u/S,S3}$, $I_{f/S,S3}$, and $I_{F/S,S3}$, which are the mass moment of inertia for the upper arm, forearm, and external load with respect to the shoulder joint using the parallel axis theorem. The joint torque θ_3 can be expressed as

$$\begin{aligned}
\tau_{3,fr} = & \left[I_{u/S,S3} + I_{f/S,S3} + I_{F/S,S3} + (m_u \zeta^2 + m_f + F_h) r_u^2 \right. \\
& + (m_f \xi^2 + F_h) r_f^2 + 2(m_f \xi + F_h) r_u r_f \left. \right] \ddot{\theta}_u \\
& - (m_u \zeta r_u + m_f r_u + F_h r_u + m_f \xi r_f + F_h r_f) g \sin \theta_u \quad (9)
\end{aligned}$$

In the frontal raise, the shoulder and elbow joints generate torque. For the shoulder flx-ext exercise using the upper limb exoskeleton, a user would use the same movement as the free-weight frontal raise motion, and the mass moments of inertia of link 3 and link 4, $I_{G3,S3}$, and $I_{G4,e3}$ would be replaced by the mass moments of inertia with respect to the shoulder joint, $I_{G3/S,S3}$, and $I_{G4/S,S3}$, by using the parallel axis theorem. Link 1 and link 2 are not involved in this motion. The joint torque of the shoulder with the exoskeleton can be expressed as

$$\begin{aligned}
M_{3,fr} = & \left[I_{u/S,S3} + I_{f/S,S3} + I_{G3/S,S3} + I_{G4/S,S3} \right. \\
& + (m_u \zeta^2 + m_f) r_u^2 + m_f \xi^2 r_f^2 + 2m_f \xi r_u r_f \\
& + 1/4m_3 l_3^2 + m_4 l_3^2 + 1/4m_4 l_4^2 + m_4 l_3 l_4 \left. \right] \ddot{\theta}_u \\
& + (m_u \zeta r_u + m_f r_u + m_f \xi r_f + 1/2m_3 l_3 \\
& + m_4 l_3 + 1/2m_4 l_4) g \sin \theta_u + (K_2 l_{SA2} - K_3 l_{SA3}) r_u \sin \theta_u \\
& - (K_2 l_{EB2} - K_3 l_{EB3}) r_u \sin \theta_u \\
& + 2(K_2 l_{EB2} l_{SA2} + K_3 l_{EB3} l_{SA3}) \sin 2\theta_u \quad (10)
\end{aligned}$$

2.4.3 Elbow Flexion/Extension

An example of the elbow flx-ext resistance exercise is the dumbbell curl motion, which is used to strengthen the biceps brachii, brachialis, and brachioradialis muscles. In the dynamic model, by using an angle θ_u equal to 0 degrees, Eq. (4) yields the moment at the elbow. $I_{f,e3}$ and $I_{F,e3}$ should be replaced by the the

mass moments of inertia with respect to the elbow joint, $I_{f/E,e3}$ and $I_{F/E,e3}$. The forearm rotates about the e_3 axis with θ_f , and the elbow joint torque can be expressed as

$$\begin{aligned}
\tau_{4,dc} = & \left[I_{f/E,e3} + I_{F/E,e3} + (m_f \xi^2 + F_h) r_f^2 \right] \ddot{\theta}_f \\
& + (m_f \xi r_f + F_h r_f) g \sin \theta_f \quad (11)
\end{aligned}$$

To train the upper limb exoskeleton for the elbow flx-ext exercise, we assume the angle θ_u equals 0 degrees, and Eq. (6) yields the moment at the elbow for the upper limb exoskeleton. $I_{f,e3}$ and $I_{G4,e3}$ should be replaced by the the mass moments of inertia with respect to the elbow joint, $I_{f/E,e3}$ and $I_{G4/E,e3}$. The joint torque of the elbow with the exoskeleton can be expressed as

$$\begin{aligned}
M_{4,dc} = & \left[I_{f/E,e3} + I_{G4/E,e3} + m_f \xi^2 r_f^2 + 1/4m_4 l_4^2 \right] \ddot{\theta}_f \\
& + (m_f \xi r_f + 1/2m_4 l_4) g \sin \theta_f \\
& - (K_2 l_{EB2} - K_3 l_{EB3}) r_u \sin \theta_f \\
& + (K_2 l_{EB2} l_{SA2} + K_3 l_{EB3} l_{SA3}) \sin \theta_f \quad (12)
\end{aligned}$$

2.5 The Prototype

A prototype of the spring-loaded upper limb exoskeleton was built based on the derived design constraints, developed embodiment design, and a detailed design from previous work [8] (Figs. 2 and 3(a)) to evaluate its basic function and its performance mechanics.

The 4-DOF kinematic chain exoskeleton contains four links. Link 1 and the posterior linkage are connected by a revolute joint at axis z_0^* . Links 1 and 2 are connected by the other revolute joint at axis z_1^* . Axes z_0^* and z_1^* are parallel to axes z_0 and z_1 , respectively, and the rotational joint angles for the z_0^* and z_1^* axes are the same as the rotational angles for the shoulder horizontal flx-ext and shoulder abd-add exercises, whereas links 2 and 3 pivot using a revolute joint at axis z_2 . For the 1-DOF elbow joint, links 3 and 4 pivot using a revolute joint at axis z_3 to accomplish the elbow flx-ext exercise. The arrangement of the three revolute joints for the 3-DOF shoulder joint is illustrated in Figs. 2 and 3(b). The revolute joints for the z_0^* , z_1^* , and z_2 axes are used to perform shoulder horizontal flx-ext, abd-add, and flx-ext movements, respectively. The elbow joint is accommodated through a revolute joint and selectable connection positions in the upper arm link that can be adjusted to accommodate small-, medium-, and large-sized people to achieve the elbow flx-ext motion. The links were primarily made of an aluminum alloy; thrust bearings were chosen to decrease defects due to clearance and to provide a frictionless rotation. The length of the forearm link is also adjusted using connection positions, which allows the device to fit different individuals, as shown in Fig. 3(a). In this design, standard springs with a wire and pulley construction were used to emulate zero-free-length springs. The zero-free-length spring K_1 is attached to point $A1$ on link 1, and point $A1$ is attached to link 2, as shown in Fig. 3(b). The standard spring K_1

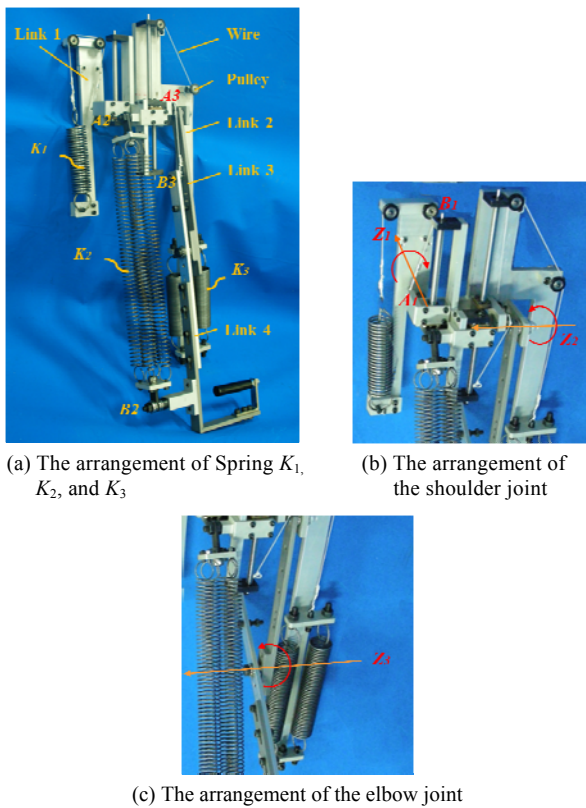


Fig. 3 The prototype of the upper limb exoskeleton

was fixed using a pin and was connected to point $B1$ and point $A1$ with wire and pulleys. The distance from point $B1$ to point $A1$ is not limited to the free length of the spring. The arrangement for the K_2 and K_3 springs is the same as for spring K_1 , as shown in Fig. 3(a). To increase the resistance intensity of the exercise, the spring connection locations $A1$, $A2$, and $A3$, which are separately integrated with nuts on the slide screws installed at link 2, could be adjusted using three slide screws to increase the resistance intensity of the exercise rather than having to change the stiffness of the springs.

This design was expected to provide low to moderate resistance to stimulate the strength of muscle recovery in patients with a variety of pathological conditions, including musculoskeletal injuries, osteoporosis, hypertension, and some chronic diseases [4] as well as to provide more intense strength training for healthy individuals. In this prototype, the maximum resistance force was designed to be 49N (corresponding to a 5kg dumbbell). Therefore, it is important to choose springs of suitable stiffnesses. In this prototype, l_{EB3} was designed to be 150mm (*i.e.*, shorter than the length of the subject's upper arm). The spring-adjustable points are limited from 1mm to 160mm. The adjustable lengths of l_{CA1} , l_{SA2} , and l_{SA3} of springs K_1 , K_2 , and K_3 were designed to be attached to link 2, which was a reasonable and convenient location for adjusting the exoskeleton. Moreover, the length of l_{P*B1} was designed to be 155mm, which conformed to the limitations of the adjustable range. Based on the limitations and the mass properties of the linkages, the anthropom-

etric parameters of humans, and the practical implementation of this design, we chose springs with the following stiffnesses from a catalog [34] of standard springs: K_1 with 1.421N/mm (0.145kgw/mm), K_2 with 0.49N/mm (0.05kgw/mm), and K_3 with 0.69N/mm (0.07kgw/mm). Detailed spring design parameters for the prototype exoskeleton are listed in Table 1.

2.6 Experiment Methods and Instrument

2.6.1 The Subjects

One healthy male and one healthy female volunteered to participate in this preliminary evaluation. The subjects self-reported no history of neural or musculoskeletal disease. Both subjects signed informed consent forms and the experiment was approved by ITRI's ethics committee. The subjects' anthropometric parameters are listed in Table 2. These parameters are adopted for the joint torque calculation in the post data analysis followed by the data collection.

2.6.2 Experimental Set-Up

Shoulder and elbow motions were recorded with a Vicon MX-F20 motion analysis system (Oxford Metrics Ltd., Oxford, UK) at a 100Hz capture rate. This system utilizes eight synchronized high-speed infrared charge-coupled display (CCD) cameras to track eight reflective markers, which measure 14mm in diameter and were mounted on predetermined bony anatomical landmarks using double-sided hypoallergenic tape. The predetermined body anatomical landmarks were located on the trunk and the upper limb of the subject, including the 7th cervical vertebrae (C7), the clavicle (CLAV), the right shoulder (RSHO), the right lateral elbow (RLEL), the right medial elbow (RMEL), the processus styloideus radius (RMWR), the processus styloideus ulna (RLWR), and the metacarpophalangeal joints (MCP) of the right middle finger (RFIN); these locations were chosen to define the segments and minimize the skin motion and are shown in Fig. 4.

An initial dynamic calibration followed by a static calibration of the motion capture system was performed prior to the experiment. Motion capture software (Vicon Nexus 1.3) was used to digitize the body landmarks. After the markers were properly attached, the subjects were asked to stand in object-space (or the capture volume) to perform a static calibration and to construct the upper limb model. The subjects were then asked to move their shoulder, elbow, and wrist joints to perform the required dynamic calibration to ensure that each marker could be seen by at least two cameras at all times during the data recording. The motion analysis system recorded the movement of the upper limb segment by tracking the 3-D location of the markers while the subject performed the selected free-weight exercises and the shoulder abduction-adduction, the shoulder flx-ext, and the elbow flx-ext movement with the spring-loaded upper limb exoskeleton in the object-space in the view of the CCD cameras.

The test of basic functions consisted of shoulder abd-add, flx-ext, and elbow flx-ext. Vicon motion data were collected from both the male and female subjects.

Table 1 Inertial parameters for the upper limb exoskeleton

Links (i)	1	2	3	4		
Mass (kg)	0.949	3.470	0.716	0.867		
Movements	abd-add (Shoulder joint)		flx-ext (Shoulder joint)		flx-ext (Elbow joint)	
Subjects	M	F	M	F	M	F
Mass moment of inertia (N-mm ²)	510,275	476,861	208,047	174,634	35,865	27,651

M: Male; F: Female

Table 2 Anthropometric parameters of the subjects used in the data analysis

TBW (kg)		Segment	Longitudinal length (mm)		Segmental weight (kg)		Sagittal r (%)		Longitudinal r (%)	
Male	Female		M	F	M	F	M	F	M	F
77	60	Upper arm	280	263	2.09	1.53	28.5	27.8	15.8	14.8
		Forearm	352	335	1.25	0.63	27.6	26.1	12.1	9.4

TBW: Total body weight; M: Male; F: Female

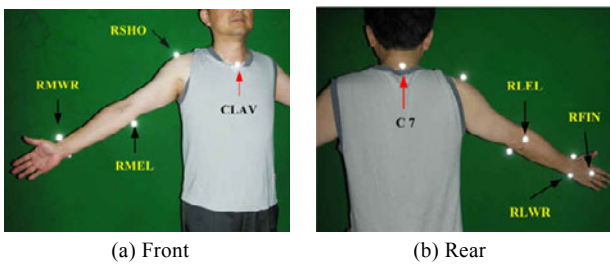


Fig. 4 Marker placement on the thorax, clavicle, and right upper limb

Table 3 lists the exact values of l_{CA1} , l_{SA2} , and l_{SA3} for the 1 kg and 3 kg weight resistances applied to the upper limb exoskeleton, which were calculated by substituting the anthropometric parameters of the male and female subjects into the design constraints obtained in the previous study. The resistance was easily changed by adjusting the position of the nut on the slide screw corresponding to the selected exercise to a new position relative to the zero position (*i.e.*, aligned with the Z_2 axis); these positions are listed in Table 3.

2.6.3 Protocols

Three common human movements—shoulder abd-add, shoulder flx-ext, and elbow flx-ext—were chosen for evaluation. Each movement was performed in a slow, controlled manner: Lifting (1 second) and lowering (1 second) without sudden jerks or acceleration. Five consecutive repetitions were performed. A metronome was employed to help the subjects maintain the tempo of their movements. The ranges of movement under evaluation are shown in Fig. 5. The 1 and 3kg dumbbells and the resistance were set for free-weight exercise and upper limb exoskeleton motion, respectively.

Table 3 The adjustable spring lengths for the 1 and 3 kg weight resistances in the experiment

Subjects	Resistance (kg)	Adjustments of springs for muscle strengthening exercises (mm)		
		Shoulder abd-add (l_{CA1})	Shoulder flx-ext (l_{SA2})	Elbow flx-ext (l_{SA3})
Male	1	5	9	15
	3	74	49	82
Female	1	4	10	14
	3	67	50	73

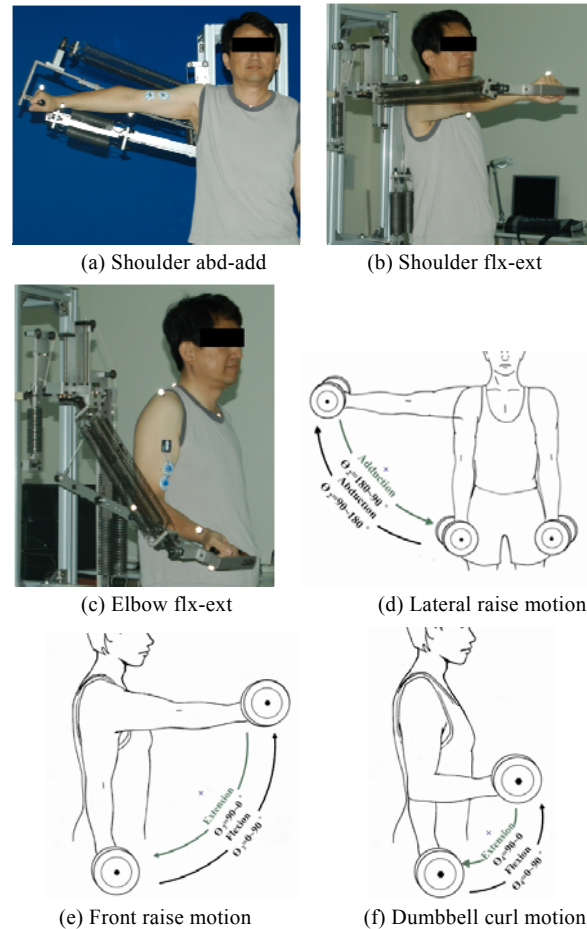


Fig. 5 Subjects performed the upper limb exoskeleton and dumbbell exercises with different

2.6.4 Data Analysis

The position of the markers during the task was recorded and the signal was then converted into a digital format for post processing. The inverse dynamics method is the most common method used to solve for an unknown reaction force and moment. The analysis begins with the most distal segment and moves upward through the kinematic chain. All of the external forces acting on the system are known. Joint torques were then calculated using a 3D generic inverse dynamics method [35]. Motion analysis data from the exercises were acquired using the Vicon Nexus software and were post processed using Matlab to convert the raw posi-

tions into useful kinematic data. Analysis of the upper limb kinetics was restricted to the motion of the shoulder and elbow. Data from the first three of the five repeated trials were analyzed to obtain an average of three results. If one of these three data sets was not acceptable for our analysis, then the fourth or fifth data set was chosen for additional analysis.

3. RESULTS AND DISCUSSION

Data collected from the preliminary evaluation shows that the movement patterns and joint torques of the shoulder abd-add, shoulder flx-ext, and the elbow flx-ext using the upper limb exoskeleton are nearly equivalent to those obtained from the upper limb dumbbell lateral raise, dumbbell frontal raise, and dumbbell curl motion. However, the shoulder joint sustains a lower inertial moment when doing the exercise with the upper limb exoskeleton.

Figure 6 compares the joint torques from the free-weight exercise and the resistance exercise of the upper limb exoskeleton based on the velocity and the effect of inertia. Generally, the dumbbell exercises generated a higher inertial moment on the shoulder joint, except for the 1kg dumbbell exercise compared with the 1kg exoskeleton resistance, as shown in Figs. 6 (a) and 6(b). We found that link 2 had a larger mass moment of inertia in the current design compared with the 1 kg dumbbell.

Figure 7 compares the mass moments of inertia calculated from the 1, 3, and 5kg fixed weight dumbbells and the exoskeleton motion of the prototype for the male and female subjects. The calculations show that

the dumbbell held at the distal end of upper limb has a larger inertial effect than the current upper limb exoskeleton prototype; moreover, as the weight of dumbbell increased, the inertial effect also increased dramatically. We also found that link 2 has a larger mass moment of inertia in the current exoskeleton design compared with the 1 kg dumbbell, which agrees with the experimental results.

These results suggest that the mass moment of inertia of the linkages should conform to certain constraints. For shoulder abd-add, by comparing the coefficient of angular acceleration $\ddot{\theta}_u$ in Eqs. (7) and (8) and incorporating the kinematic design constraints obtained in the previous study, the inequality equation $I_{G2/S,S3} + I_{G3/S,S3} + I_{G4/S,S3} + m_2 l_2^2 + 1/4 m_3 l_3^2 + m_4 l_3^2 + 1/4 m_4 l_4^2 + m_4 l_3 l_4 < I_{F/S,S3} + F_h (r_u + r_f)^2$ should be maintained to ensure that less dynamic joint torque is created by the exoskeleton movement compared with the free-weight exercise. By applying the same procedures, the inequality equations for shoulder flx-ext and elbow flx-ext can be obtained as additional design constraints for the exoskeleton design.

4. CONCLUSIONS

In this study, a dynamic model of a spring-loaded upper limb exoskeleton and additional design constraints are proposed. A prototype was constructed to perform a preliminary evaluation of shoulder abd-add,

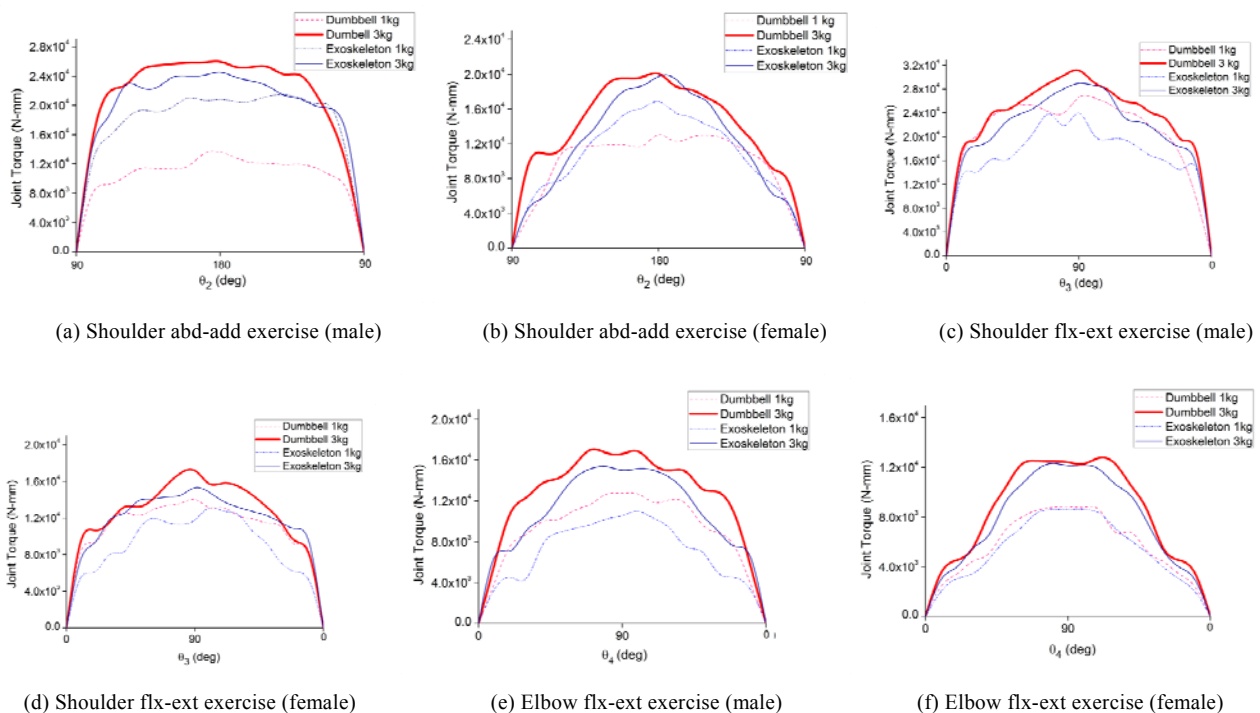


Fig. 6 The experimental data of joint torques with 1 and 3kg resistance with the inertial effect

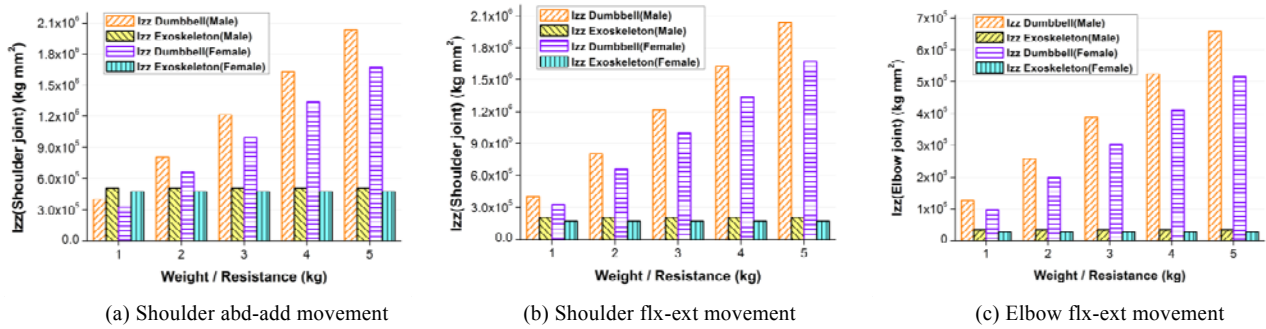


Fig. 7 Comparisons of the mass moments of inertia effect caused by the dumbbell or the exoskeleton motion

shoulder flx-ext, and elbow flx-ext exercises as well. The shoulder and elbow joint torques are expected to have smaller inertial forces when using the exoskeleton compared with the joint torques obtained from free-weight exercises. The in-line motion of two subjects using free weights and the upper limb exoskeleton was recorded and analyzed. The motions during all the exercises showed good consistency. Based on these results, this work provides a dynamic model and a working prototype of an upper limb exoskeleton with an adjustable upper arm and forearm length suitable for average-sized human beings. By arranging small-inertia springs, the device is capable of reducing unfavorable lengthening of the muscles during high-intensity free-weight exercises or joint overload caused by large inertial moments. Further research using a broader assessment is warranted to confirm and expand on these results.

REFERENCES

1. Kraemer, W. J. and Ratamess, N. A., "Fundamentals of Resistance Training: Progression and Exercise Prescription," *Medicine & Science in Sports & Exercise*, **36**, pp. 674–688 (2004).
2. American College of Sports Medicine, "Position Stand: Progression Models in Resistance Training for Healthy Adults," *Medicine & Science in Sports & Exercise*, **34**, pp. 364–380 (2002).
3. Williams, M. A., Haskell, W. L., Ades, P. A., Amsterdam, E. A., Bittner, V., Franklin, B. A., Gulanick, M., Laing, S. T. and Stewart, K. J., "Resistance Exercise in Individuals with and Without Cardiovascular Disease: 2007 update," *Circulation*, **116**, pp. 572–584 (2007).
4. Taylor, N. F., Dodd, K. J. and Damiano, D. L., "Progressive Resistance Exercise in Physical Therapy: A Summary of Systematic Reviews," *Physical Therapy*, **85**, pp. 1208–1223 (2005).
5. Risser, W. L., "Weight-Training Injuries in Children and Adolescents," *American Family Physician*, **44**, pp. 2104–2110 (1991).
6. Kerr, Z. Y., Collins, C. L. and Comstock, R. D., "Epidemiology of Weight Training-Related Injuries Presenting to United States Emergency Departments, 1990 to 2007," *The American Journal of Sports Medicine*, **38**, pp. 765–771 (2010).
7. Lavallee, M. E. and Balam, T., "An Overview of Strength Training Injuries: Acute and Chronic," *Current Sports Medicine Report*, **9**, pp. 307–313 (2010).
8. Wu, T. M., Wang, S. Y. and Chen, D. Z., "Design of an Exoskeleton for Strengthening the Upper Limb Muscle for Overextension Injury Prevention," *Mechanism and Machine Theory*, **46**, pp. 1825–1839 (2011).
9. Buckley, M. A., Yardley, A., Johnson, G. R. and Carus, D. A., "Dynamics of the Upper Limb During Performance of the Tasks of Everyday Living-A Review of the Current Knowledge Base," *Proceedings of the IMechE*, **210**, pp. 241–247 (1996).
10. Myer, K., *Biomedical Engineering and Design Handbook*, 2nd Edition, McGraw-Hill, New York pp. 195–210 (2009).
11. Hollerbach, J. M. and Flash, T., "Dynamic Interactions Between Limb Segments During Planar Arm Movement," *Biological Cybernetics*, **44**, pp. 67–77 (1982).
12. Nef, T., Mihelj, M. and Riener, R., "ARMin: A Robot for Patient-Cooperative Arm Therapy," *Medical and Biological Engineering and Computing*, **45**, pp. 887–900 (2007).
13. Nagarsheth, H. J., Savsani, P. V. and Patel, M. A., "Modeling and Dynamics of Human Arm," *4th IEEE Conference on Automation Science and Engineering*, Washington, pp. 924–928 (2008).
14. Apkarian, J., Naumann, S. and Cairns, B., "A Three-Dimensional Kinematic and Dynamic Model of the Lower Limb," *Journal of Biomechanics*, **22**, pp. 143–155 (1989).
15. Requejo, P. S., Wahl, D. P., Bontrager, E. L., Newsam, C. J., Gronley, J. K., Mulroy, S. J. and Perry, J., "Upper Extremity Kinetics During Lofstrand Crutch-Assisted Gait," *Medical Engineering & Physics*, **27**, pp. 19–29 (2005).
16. Thomas, J. S., Corcos, D. M. and Hasan, Z., "Kinematic and Kinetic Constraints on Arm, Trunk, and Leg Segments in Target-Reaching Movement," *Journal of Neurophysiology*, **93**, pp. 352–364 (2005).
17. Shemmell, J., Corcos, D. M. and Hasan, Z., "Kinetic and Kinematic Adaptation to Anisotropic Load," *Experimental Brain Research*, **192**, pp. 1–8 (2009).

18. Nagano, A., Yoshioka, S., Komura, T., Himeno, R. and Fukashiro, S., "A Three-Dimensional Linked Segment Model of the Whole Human Body," *International Journal of Sport & Health Science*, **3**, pp. 311–325 (2005).
19. AbdulRahman, S. A., Rambely, A. S. and Ahmad, R. R., "A Biomechanical Model Via Kane's Equation—Solving Trunk Motion with Load Carriage," *American Journal of Scientific Industrial Research*, **2**, pp. 678–685 (2011).
20. Anglin, C. and Wyss, U. P., "Review of Arm Motion Analyses," *Proceedings of the Institution of Mechanical Engineers; Part H; Journal of Engineering Medicine*, **214**, pp. 541–555 (2000).
21. Richards, J. G., "The Measurement of Human Motion: A Comparison of Commercially Available System," *Human Movement Science*, **18**, pp. 589–602 (1999).
22. Zhou, H. and Hu, H., "Human Motion Tracking for Rehabilitation—A Survey," *Biomedical Signal Process Control*, **3**, pp. 1–18 (2008).
23. Cappozzo, A., Croce, U. D., Leardini, A. and Chiari, L., "Human Movement Analysis Using Stereophotogrammetry Part 1: Theoretical Background," *Gait & Posture*, **21**, pp. 186–196 (2005).
24. Chiari, L., Croce, U. D., Leardini, A. and Cappozzo, A., "Human Movement Analysis Using Stereophotogrammetry Part 2: Instrumental Errors," *Gait & Posture*, **21**, pp. 197–211 (2005).
25. Leardini, A., Chiari, L., Croce, U. D. and Cappozzo, A., "Human Movement Analysis Using Stereophotogrammetry Part 3: Soft Tissue Artifact Assessment and Compensation," *Gait & Posture*, **21**, pp. 212–225 (2005).
26. Croce, U. D., Leardini, A., Chiari, L. and Cappozzo, A., "Human Movement Analysis Using Stereophotogrammetry Part 4: Assessment of Anatomical Landmark Misplacement and Its Effects on Joint Kinematics," *Gait & Posture*, **21**, pp. 226–237 (2005).
27. Schmidt, R., Disselhorst-Klug, C., Silny, J. and Rau, G., "A Marker-Based Measurement Procedure for Unconstrained Wrist and Elbow Motions," *Journal of Biomechanics*, **32**, pp. 615–621 (1999).
28. Biryukova, E. V., Roby-Brami, A., Frolov, A. A. and Mokhtari, M., "Kinematics of Human Arm Reconstructed From Spatial Tracking System Recordings," *Journal of Biomechanics*, **33**, pp. 985–995 (2000).
29. Prokopenko, R. A., Biryukova, E. V., Roby-Brami, A. and Frolov, A. A., "Assessment of the Accuracy of a Human Arm Model with Seven Degrees of Freedom," *Journal of Biomechanics*, **34**, pp. 177–185 (2001).
30. Hingtgen, B., McGuire, J. R., Wang, M. and Harris, G. F., "An Upper Extremity Kinematic Model for Evaluation of Hemiparetic Stroke," *Journal of Biomechanics*, **39**, pp. 681–688 (2006).
31. <http://www.vicon.com/>
32. Romilly, D. P., Anglin, C., Gosine, R. G., Hershler, C. and Raschke, S. U., "A Functional Task Analysis and Motion Simulation for the Development of a Powered Upper-Limb Orthosis," *IEEE Transactions on Rehabilitation Engineering*, **2**, pp. 119–129 (1994).
33. DeLeva, P., "Adjustments to Zatsiorsky-Seluyanov's Segment Inertia Parameters," *Journal of Biomechanics*, **29**, pp. 1223–1230 (1996).
34. The Stock Precision Engineered Components (SPEC), Associated Spring, [Online]. Available: <http://springming.sobuy.com/ezfiles/springming/img/img/61161/SPEC-04E.pdf>.
35. Dumas, R., Aissaoui, R. and De Guise, J. A., "A 3D Generic Inverse Dynamic Method Using Wrench Notation and Quaternionalgebra," *Computer Methods in Biomechanics and Biomedical Engineering*, **7**, pp. 159–166 (2004).

(Manuscript received September 27, 2011, accepted for publication March 8, 2012.)